ANTICANCER RESEARCH *42*: 5773-5781 (2022)
doi:10.21873/anticanres.16084

COX-2 Acts as a Key Mediator of Trifluoperazine-induced Cell Death in U87MG Glioma Cells

JUYEONG PARK*, JOO YEON JEONG* and SANG SOO KANG

Department of Anatomy & Convergence Medical Science, Institute of Health Science, College of Medicine, Gyeongsang National University, Jinju, Republic of Korea

Abstract. *Background/Aim: Glioblastoma multiforme (GBM) is one of the most common brain tumors with a poor prognosis. Previously, we reported that trifluoperazine (TFP), a well-known antipsychotic, has anti-glioma activity through the modulation of intracellular calcium levels. The present study aimed to investigate the anti-cancer mechanism of action of TFP on glioma cells. Materials and Methods: The effect of TFP on U87MG cells was examined using a viability assay, flow cytometry, enzyme-linked immunosorbent assay, quantitative real-time PCR, western blot analysis, colony formation, and immunocytochemistry. Results: TFP treatment decreased cell viability. To test the possible involvement of COX-2 in the anti-cancer activity of TFP on U87MG cells, a COX-2 inhibitor was applied. COX-2 inhibitor pretreatment restored TFP-induced reduction in viability to the control level. Additionally, TFP-induced changes in the apoptotic cell population, production of prostaglandins (PGE_2, PGD_2, 15d-PGJ_2), and nuclear translocation of peroxisome proliferator-activated receptor γ (PPARγ) were ameliorated by COX-2 inhibitor pretreatment. Conclusion: TFP suppressed the proliferation of U87MG glioma cell in a COX-2/PPARγ-dependent manner.*

Glioblastoma multiforme (GBM) is a malignant brain tumor derived from glial cells. The prognosis of patients is very low. Median survival is less than 10 months. GBM treatment usually involves surgery, radiation therapy, and chemotherapy with temozolomide. However, the expected survival rate extension is only several months even with these treatments (1). Therefore, it is important to develop new drugs for GBM treatment that can increase the survival rate without side effects.

The development of new drugs requires a lot of time and money. Therefore, drug repositioning that uses the originally discovered drugs for other diseases is increasing (2, 3). Recently, as an extension of drug repositioning, it has been confirmed that cancer incidence decreases when antipsychotics are administered (4-6). Among them, trifluoperazine (TFP) has been widely used to treat schizophrenia. TFP has also been shown to inhibit the growth of lung cancer stem cells (7), induce cell death in pancreatic ductal carcinoma (8), and suppress the metastasis of melanoma (9) and breast cancer (10). In previous reports, we demonstrated that TFP suppressed the viability and growth of glioma cells *via* increasing intracellular Ca^{2+} levels (11, 12).

Despite the several reported studies, the underlying mechanisms of the TFP-induced intracellular Ca^{2+} increase and cancer cell death remain unresolved. Here, we aimed to identify the mechanism of action of TFP-induced cell death.

Cyclooxygenase-2 (COX-2) is well known as an enzyme that synthesizes prostaglandins (PGs) associated with inflammation and pain. Recently, COX-2 has been shown to affect proapoptotic mechanisms (13-15). Furthermore, it has been reported that apoptosis is induced by COX-2 and peroxisome proliferator-activated receptor γ (PPARγ) in lung cancer cells (16). PPARγ is a nuclear receptor that functions in many physiological processes, including lipid metabolism, cell growth, and apoptosis (17). PPARγ can induce apoptosis of cancer cells (18). The present study investigated the potential contribution and coordinated action of COX-2 and PPARγ in the TFP-induced apoptosis of human glioma cells.

Materials and Methods

Cell culture. U87MG, U251MG, and T98G cells were purchased from the American Type Culture Collection and cultured in Dulbecco's Modified Eagle's Medium supplemented with 10% fetal

*These Authors contributed equally to this study.

Correspondence to: Sang Soo Kang, Ph.D., Department of Anatomy and Convergence Medical Science, Institute of Health Sciences, College of Medicine, Gyeongsang National University, 15 Jinju-daero 816 Beon-gil, Jinju, Gyeongnam 52727, Republic of Korea. Tel: +82 557728033, Fax: +82 557728039, e-mail: kangss@gnu.ac.kr

Key Words: Glioblastoma multiforme, Trifluoperazine, COX-2, PPARγ.

bovine serum, penicillin (100 units/ml), and streptomycin (100 μg/ml) in a humidified 5% CO_2 incubator at 37˚C. All culture media and supplements were obtained from Gibco (Grand Island, NY, USA).

Cell viability assay. Cell viability was measured by the methylthiazoltetrazolium (MTT, Sigma-Aldrich, St. Louis, MO, USA) assay. Cells were seeded in 96-well plates at a density of 2×10^3 cells per well. After overnight incubation, cells were treated with TFP (Sigma-Aldrich) for 48 h. After treatments, 100 μl of MTT (1 mg/ml) was added to the medium for 2 h. The cells were solubilized with dimethyl sulfoxide (Amresco, Solon, OH, USA), and absorbance was measured at 570 nm with Infinite M200 Pro (Tecan, Mannedorf, Switzerland).

Cell cycle analysis. U87MG cells (1×10^6 cells) were cultured in 100-mm dish and treated with TFP for 48 h. Cell cycle analysis was performed with Click-iT® EdU Flow Cytometry Assay Kit (Invitrogen, Carlsbad, CA, USA), according to the manufacturer's instructions. SYTOX® AADvanced™ dead cell stain (Invitrogen) was used to stain the DNA for the analysis of the cell cycle. Flow cytometry was performed using the Attune NxT flow cytometer (Thermo Fisher Scientific, Rockford, IL, USA).

DNA fragmentation assay. U87MG cells were grown for 12 h in 6-well plates. Briefly, cells were harvested, and then incubated in an Eppendorf tube with TFP for 4 h at 37˚C. The cell pellets were collected, and DNA fragmentation was analyzed using the Cell Death Detection enzyme-linked immunosorbent assay (ELISA) kit (Roche Diagnostics, Mannheim, Germany) according to the manufacturers' guidelines.

Quantitative real-time PCR (qPCR). RNA was isolated with Trizol reagent (Invitrogen) and 1 μg of it was reverse transcribed for the synthesis of cDNA. The mRNA expression of COX-2 was evaluated by qPCR. qPCR was performed using TOPreal (Enzynomics, Daejeon, Republic of Korea) in a Light Cycler 480 II (Roche Life Science, Indianapolis, IN, USA). qPCR primer pairs were as follows: COX-2, forward: TGGTGCCTGGTCTGATGATG and reverse: GCCTGCT TGTCTGGACAAC. GAPDH, forward: GCACCCCTGGCCAA GGTCAT and reverse: ACGCCACAGTTTCCCGGAGG.

Western blotting. U87MG cells were lysed in radioimmunoprecipitation assay buffer (Thermo Fisher Scientific) containing 25 mM Tris-HCl pH 7.6, 150 mM NaCl, 1% NP-40, 1% sodium deoxycholate, 0.1% SDS, protease inhibitor cocktail (Roche) and phosphatase inhibitor cocktail (GenDepot, Barker, TX, USA). Equivalent amounts of total protein (20 μg) were separated by SDS-PAGE on 8% polyacrylamide gels and then transferred to nitrocellulose membranes (Bio-Rad Laboratories, Hercules, CA, USA). The membrane was blocked with 5% skim milk in tris-buffered saline (TBS) containing 0.1% Tween-20 and then incubated with anti-COX-2 (Cell signaling, Beverly, MA, USA, #4842) or anti-β-actin (Sigma-Aldrich, A5441). The immunoreactivity was detected by ECL (Thermo Fisher Scientific) using LAS 4000 (Fujifilm, Tokyo, Japan).

Treatment of inhibitors. U87MG cells were grown for 12 h. COX-2 inhibitor NS398 (Sigma-Aldrich) or PPARγ inhibitor GW9662 (Sigma-Aldrich) were added to cells 1 h before TFP treatment.

Soft agar colony formation assay. U87MG cells (5×10^3 cells/well) were seeded in 6-well plates in 0.35% top agar overlaying a 0.5% base agar. The solidified cell layer was filled with medium including TFP, NS398, or GW9662, which was refreshed every 3 days. Cells were incubated at 37˚C for 2 weeks to allow colonies to develop. The colonies were stained with crystal violet and photographed.

Colony formation assay. U87MG cells (5×10^3 cells/well) were seeded in 6-well plates. The plates were incubated with TFP, NS398 or GW9662. The medium was refreshed every 3 days. Cells were incubated at 37˚C for 8 days to allow colonies to develop. The colonies were stained with crystal violet and photographed with a digital camera manually counted.

Apoptosis assay. U87MG cells (1×10^6 cells) were cultured in 100-mm dishes and treated with TFP, NS398 or GW9662 for 12 h. After treatment, cells were harvested, washed with 1 X PBS (plus 1% BSA, 2 mM EDTA), and stained with Annexin V-FITC Apoptosis detection kit (Thermo Fisher Scientific). We analyzed apoptotic cells by flow cytometry using the Attune NxT flow cytometer (Thermo Fisher Scientific).

Measurement of PGs. U87MG cells (3×10^4 cells/well) were grown for 12 h in 24-well plates. Cells were treated with TFP and NS398 for 24 h. Cell culture medium was collected and analyzed for PGE_2, PGD_2 (Cayman Chemical, Ann Arbor, MI, USA), and 15d-PGJ_2 (Enzo Life Sciences, Farmingdale, NY, USA) using ELISA kits, according to the manufacturer's instructions.

Immunocytochemistry. Cells were fixed with 4% paraformaldehyde and permeabilized with 0.1% Triton X-100. Subsequently, fixed cells were incubated with anti-PPARγ (Cell signaling, #2435) and anti-lamin A/C (Santa Cruz biotechnology, Dallas, TX, USA, sc-7292) to detect cells. Secondary antibodies were goat anti-rabbit Alexa Fluor® 488 labeled IgG for detection of PPARγ and a goat anti-mouse Alexa Fluor® 594 labeled IgG for detection of lamin A/C. The fluorescence pictures were captured using BX51-DSU microscopy (Olympus IX81, Tokyo, Japan).

Statistical analysis. All data are shown as the mean±standard error (S.E.). Data were analyzed with GraphPad Prism (La Jolla, CA, USA). Significance was determined using the unpaired student's *t*-test and one-way analysis of variance (ANOVA) plus *post hoc* Dunnett's post-test or Tukey's multiple comparison test. *p*-Values <0.05 were considered statistically significant.

Results

TFP inhibits cell viability and induces cell death in glioma cells. To evaluate the effect of TFP on glioma cell viability, MTT assay was performed. Cells were treated with TFP at various concentrations (0, 1, 2, 5, 10, and 20 μM) for 48 h. TFP reduced cell viability in all glioma cells (Figure 1A). Among three glioma cells, U87MG cells were selected for further experiments because of its common use and representative responsiveness to TFP. Since treatment with 10 μM TFP suppressed nearly 40% of U87MG cell viability, following experiments were performed at this concentration. In order to elucidate whether the reduced cell viability caused by TFP treatment is a result of the induction of cell death or inhibition of proliferation, we performed cell cycle analysis and DNA

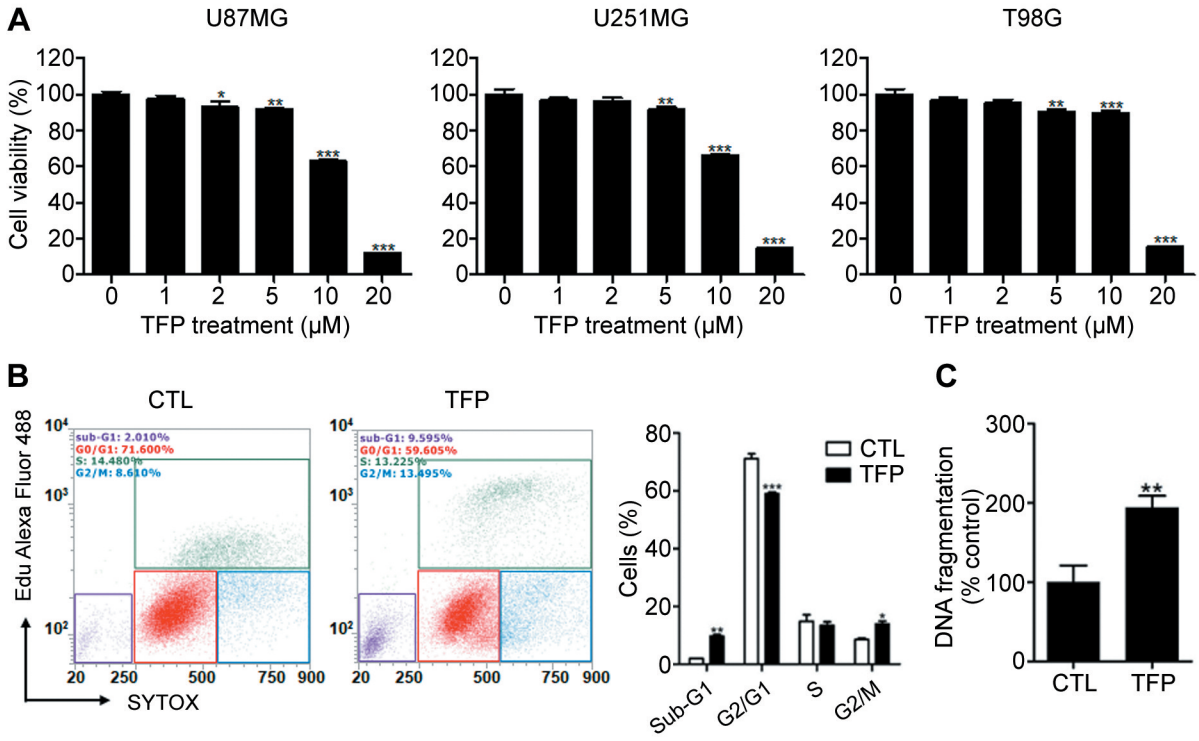

Figure 1. *Effects of TFP on U87MG cell viability and cell death. (A) U87MG, U251MG, and T98G cells were treated with TFP at concentrations ranging from 0 to 20 μM for 48 h, and cell viability was determined using MTT assay. Data are represented as mean±S.E. *p<0.05, ***p<0.001 vs. CTL. (B) Cell cycle analyses of U87MG cells treated with TFP at 10 μM for 48 h. *p<0.05, **p<0.01, ***p<0.001 vs. CTL. (C) DNA fragmentation analyses of U87MG cells. TFP was used at 10 μM for 4 h. Data are presented as mean±S.E. **p<0.01 vs. CTL.*

fragmentation assay. TFP treatment significantly increased sub-G1 and G2/M and decreased G0/G1 population of U87MG cells (Figure 1B). Furthermore, TFP treatment induced DNA fragmentation (Figure 1C). The results indicate that TFP treatment inhibits the cell cycle and induces cell death.

TFP increases COX-2 expression in U87MG cells. Some studies have reported that increased COX-2 expression is related to cancer cell apoptosis (19-21). Thus, we examined the effects of TFP treatment on the expression of COX-2 in U87MG cells. Results using qPCR showed that TFP treatment increased the mRNA levels of COX-2 (Figure 2A). The mRNA level was significantly elevated at 6 h after TFP treatment, reached a maximum level at 12 h, and remained high until 24 h although slightly reduced compared to the 12-h time point. Western blot analysis showed that the COX-2 protein levels increased in a time-dependent manner after TFP treatment. Elevated COX-2 protein levels were observed at 24 h after TFP treatment and remarkably high expression levels were reached at 48 h (Figure 2B). These results indicate that mRNA and protein expression of COX-2 are increased by TFP treatment.

COX-2 inhibitor recovers the effects of TFP on U87MG cells. To reveal the possible involvement of COX-2 in the TFP-induced decrease in cell viability, we applied the specific COX-2 inhibitor NS398. Pretreatment with NS398 reduced the increased COX-2 protein levels induced by TFP (Figure 3A) and restored the reduced cellular viability caused by TFP treatment. However, NS398 alone did not affect U87MG cell viability (Figure 3B). These results demonstrated that TFP suppressed U87MG cell viability, at least in part, *via* the COX-2 pathway. In addition, NS398 treatment also restored the reduced anchorage-dependent and anchorage-independent colony formation of U87MG cells by TFP (Figure 3C). Furthermore, the TFP-induced increase in apoptotic cell populations was also significantly reduced by NS398 treatment (Figure 3D). This result strongly demonstrates that the anti-tumorigenic activity of TFP is mediated by COX-2.

COX-2 inhibitor ameliorated the TFP-induced increased release of PGs and suppressed PPARγ nuclear translocation. We investigated whether TFP affects COX-2-related PG release. As shown in Figure 4A, TFP treatment significantly

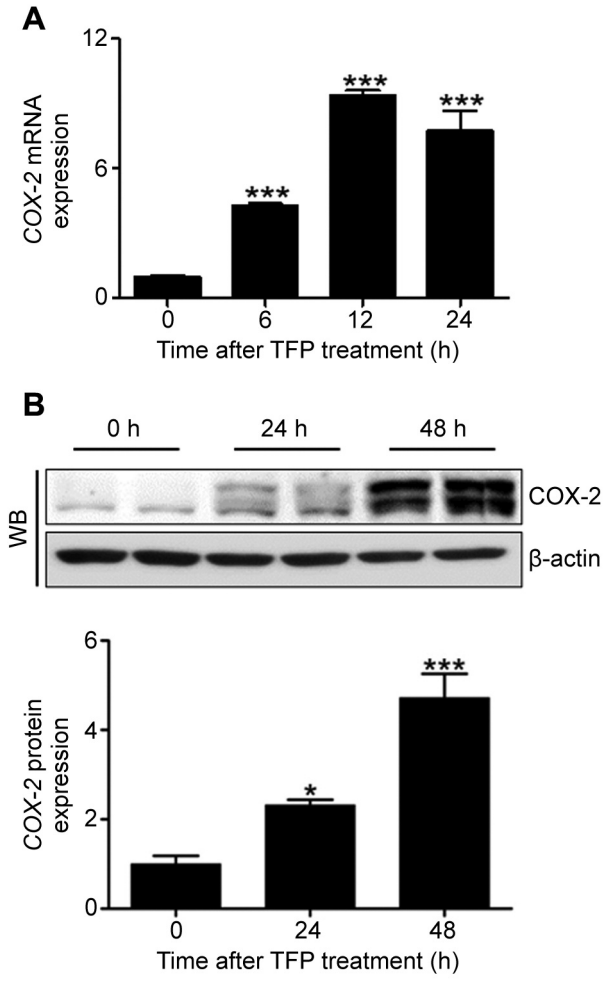

Figure 2. *Effects of TFP on COX-2 expression. (A) U87MG cells were treated with TFP at 10 μM for 6, 12, and 24 h. COX-2 mRNA expression levels were determined by qPCR. Data are represented as mean±S.E. **p<0.01, ***p<0.001 vs. CTL. (B) U87MG cells were treated with TFP at 10 μM for 24 and 48 h. The protein levels of COX-2 were examined by western blot. β-actin was used as the loading control.*

increased the release of PGE_2, PGD_2, and 15d-PGJ_2 in U87MG cells. Pretreatment with NS398 clearly suppressed the increased release of PGE_2, PGD_2, and 15d-PGJ_2.

Several studies have indicated that COX-2-derived PGE_2, PGD_2, and 15d-PGJ_2 induced COX-2-dependent apoptosis through activating the transcription factor PPARγ. PGE_2, PGD_2, and 15d-PGJ_2 are endogenous ligands of PPARγ and involved in the apoptosis of cancer cells (18, 22). Using immunocytochemistry, we showed the nuclear translocation of PPARγ as an indicator of PPARγ activation. TFP treatment evoked nuclear translocation of PPARγ, and this translocation was significantly inhibited by NS398 (Figure 4B). These results suggested that PGs and PPARγ activation are associated with COX-2-dependent apoptosis.

Impact of PPARγ on TFP-induced cell death. To determine whether PPARγ is a key mediator of TFP-induced U87MG cell death, we applied a PPARγ inhibitor (GW9662). The TFP-induced reduction in cell viability and colony formation, and the increase in apoptotic cell population were recovered by GW9662 co-treatment (Figure 5). These findings revealed that the induction of COX-2 expression and subsequent activation of PPARγ by COX-2-derived PGs as key events in the proapoptotic action of TFP on U87MG cells.

Discussion

The present study aimed to identify the underlying mechanism of TFP-induced intracellular Ca^{2+} increase and cell death in glioma cells. Previous reports have demonstrated that TFP has anti-cancer activity on several cancers including glioma (10-12, 22-25). However, to the best of our knowledge, there is no report on how TFP induces cancer cell death, especially in glioma.

Among antipsychotics, TFP has long been used for the treatment of schizophrenia (6, 26). Notably, cancer incidence is low in schizophrenia patients who have received antipsychotic treatment (27). Furthermore, several studies have shown that TFP has anti-tumor effects in many cancers (28-30). Since TFP, as an antipsychotic drug, can cross the blood-brain barrier, it may possibility be used for the treatment of GBM (31).

In our previous study, we showed that TFP directly interacts with the Ca^{2+} binding protein calmodulin (CaM) subtype 2 (32), triggering the irreversible release of Ca^{2+} by inositol 1,4,5-triphosphate receptor subtypes 1 and 2, and resulting in the inhibition of motility, invasion, and viability of GBM cells *in vitro* (11). CaM antagonists can induce apoptosis in GBM cells (33). Thus, it is possible that TFP induces GBM cell apoptosis as a CaM antagonist. However, the precise mechanism of action of TFP requires further evaluation.

It has been shown that an increase in Ca^{2+} levels activates COX-2. Treatment with the calcium ionophore, ionomycin, resulted in a significant induction of COX-2 mRNA and protein levels (34). Diosgenin, a component of plant extracts, induced cell cycle arrest and apoptosis in erythroleukemia cells through intracellular Ca^{2+} increase and COX-2 over-expression (35). As expected, TFP treatment remarkably increased the expression of COX-2 in U87MG cells (Figure 2). Although there were many controversies, COX-2 is known to be involved in cell death (36-39). Thus, we hypothesized that COX-2 might mediate the anti-cancer effect of TFP on glioma cell death. Treatment with a COX-2 inhibitor reversed the changes induced by TFP treatment, including the increased expression of COX-2, reduced cell viability, decreased colony formation, and increased apoptotic cell population. From these results, we could conclude that COX-2 is an important mediator of TFP-induced cell death in U87MG cells.

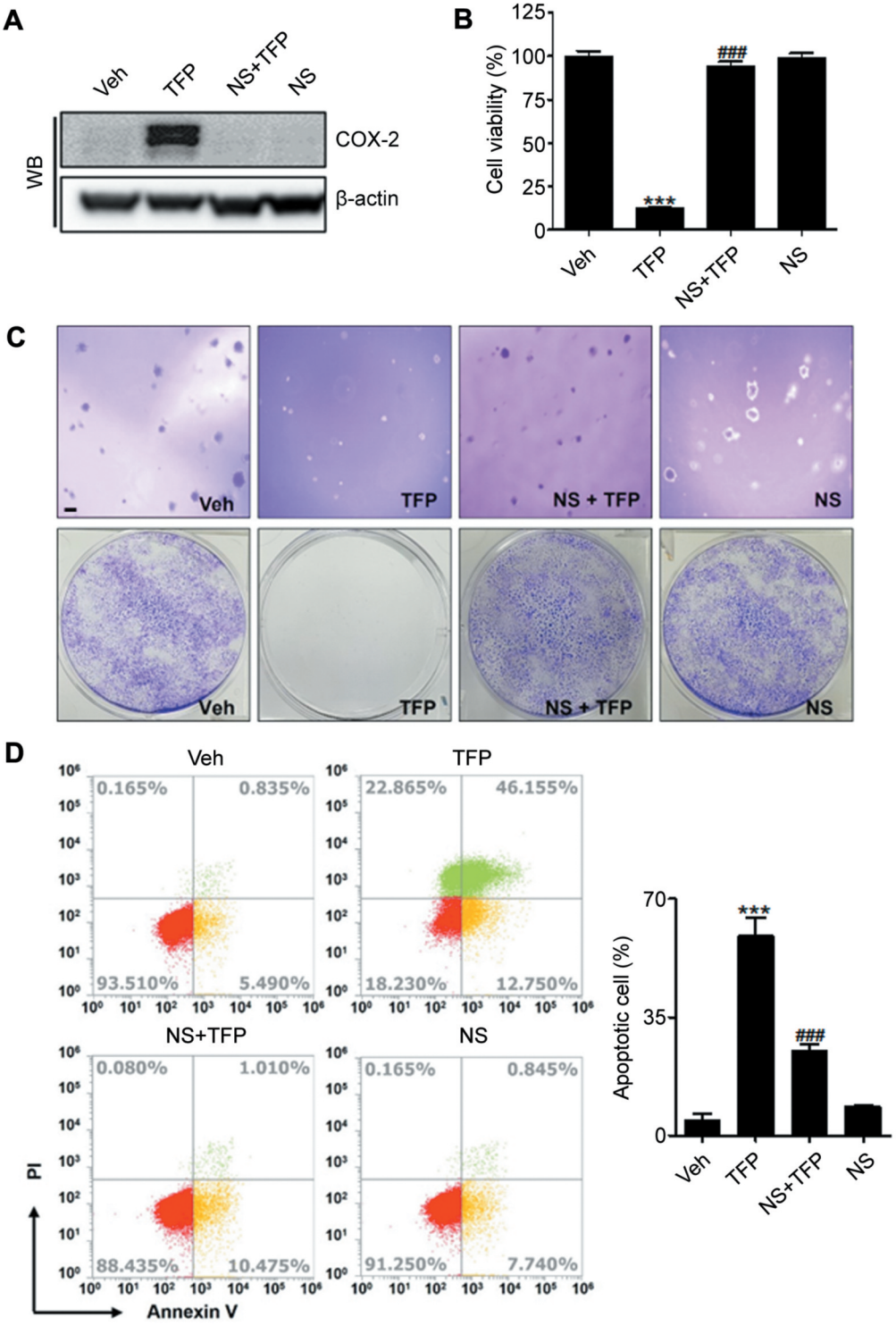

Figure 3. *Effects of NS398 on the TFP-induced suppression of U87MG cell viability. (A) U87MG cells were pretreated with or without the COX-2 inhibitor NS398 (1 μM) for 1 h, and then additionally treated with 10 μM TFP for 48 h. COX-2 protein expression was determined by western blot. β-actin was used as the loading control. (B) U87MG cells were pretreated with or without NS398 (1 μM) for 1 h, and then additionally treated with 10 μM TFP for 48 h. Cell viability was determined using the MTT assay. Data are presented as mean±S.E. ***p<0.001 vs. Vehicle (Veh), ###p<0.001 vs. TFP. (C) Colony formation of U87MG cells was determined using an anchorage-independent/-dependent colony formation assay. Scale bar represents 200 μm. (E) U87MG cells were pretreated with or without NS398 for 1 h, and then treated with 10 μM TFP for 48 h. Flow cytometry analysis of Annexin-V and propidium iodide (PI) staining of U87MG cells. Data are presented as mean±S.E. ***p<0.001 vs. Veh, ###p<0.001 vs. TFP.*

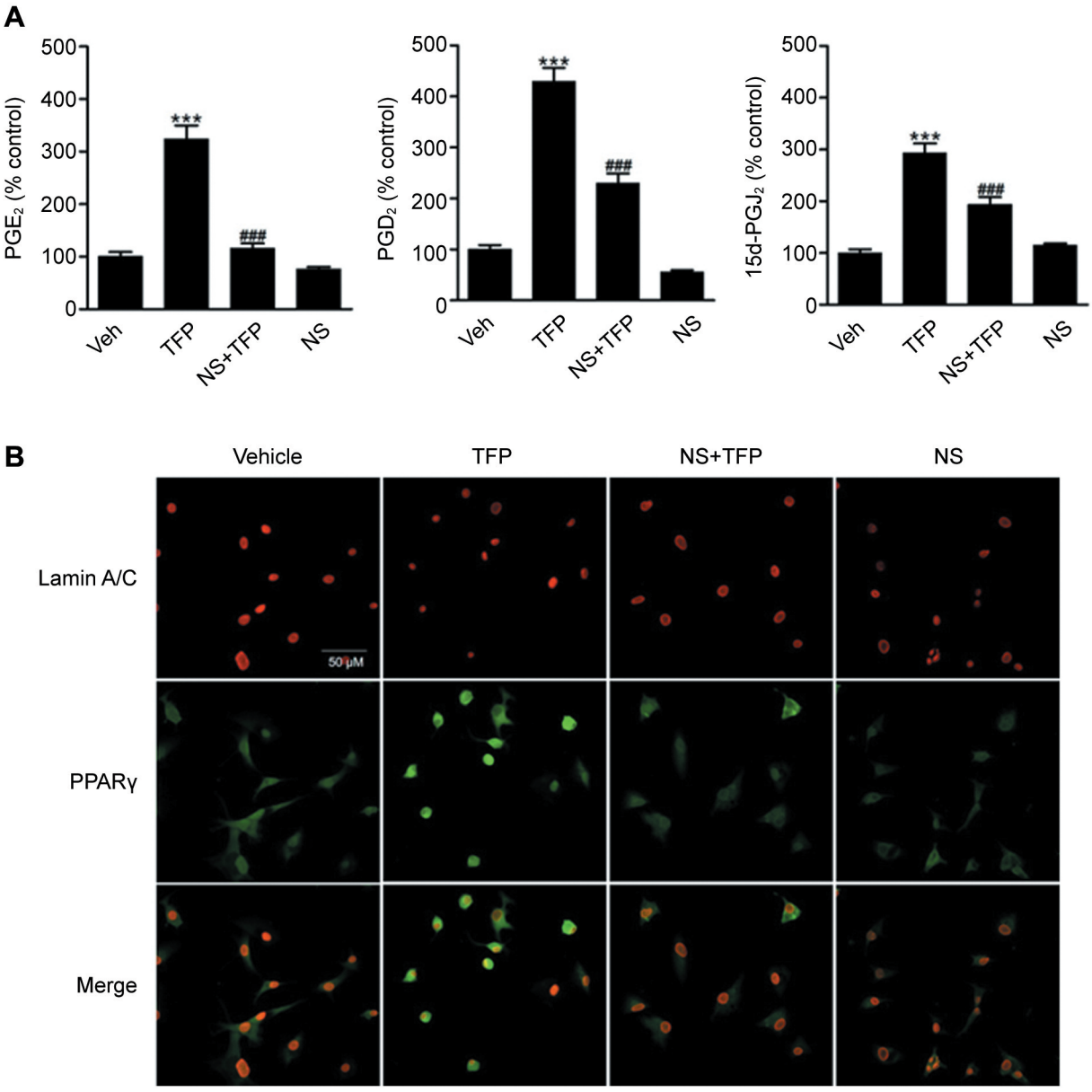

Figure 4. *Effects of NS398 in PPARγ activation by TFP. (A) U87MG cells were pretreated with or without NS398 (1 μM) for 1 h, and then treated with 10 μM TFP for 24 h. PGs levels were determined by ELISA. Data are presented as mean±S.E. ***p<0.001 vs. Vehicle (Veh), ###p<0.001 vs. TFP. (B) U87MG cells were pretreated with or without NS398 for 1 h, and then treated with 10 μM TFP for 24 h. Representative image of lamin A/C (red) and PPARγ (green) positive immunocytochemical staining. Scale bar represents 50 μm.*

COX-2 produces PGH_2, a precursor of many other biologically significant PGs. PGs are known to be involved in the inflammatory response and cell viability (40). PGE_2 induced apoptotic cell death in human leukemia cells (41) and fibroblasts (42). PGD_2 and PGJ_2 were found to be involved in apoptosis in leukemia cells (43). Recent studies have shown that COX-2-dependent PGD_2 and 15d-PGJ_2 activated PPARγ and caused apoptosis of lung cancer cells (18, 22). Based on these, we hypothesized that TFP treatment up-regulated COX-2, then increased PGs production, and eventually activated PPARγ nuclear translocation in U87MG cells.

Since PPARγ is a nuclear receptor protein, the translocation of PPARγ from the cytoplasm to the nucleus is important for its activation. We revealed the nuclear translocation of PPARγ with immunocytochemistry after TFP treatment. As shown in Figure 4, COX-2 inhibitor

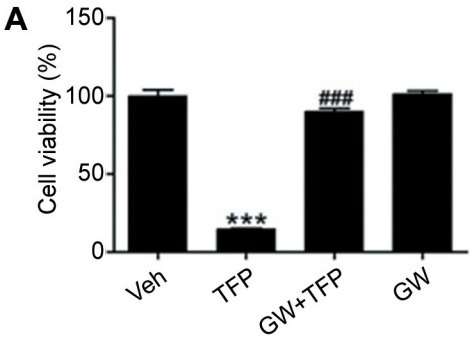

Figure 5. *Effects of GW9662 on the TFP-induced suppression of U87MG cell viability. (A) U87MG cells were pretreated with or without GW9662 (10 μM) for 1 h, and then treated with 10 μM TFP for 48 h. Cell viability was determined using a MTT assay. Data are presented as mean±S.E. ***p<0.001 vs. Vehicle (Veh), ###p<0.001 vs. TFP. (B) Colony formation of U87MG cells was determined using an anchorage-independent colony formation and anchorage-dependent colony formation. Scale bar represents 200 μm. (C) U87MG cells were pretreated with or without GW9662 for 1 h, and then treated with 10 μM TFP for 48 h. Flow cytometry analysis of Annexin-V and PI staining of U87MG cells. Data are presented as mean±S.E. ***p<0.001 vs. Veh, ###p<0.001 vs. TFP.*

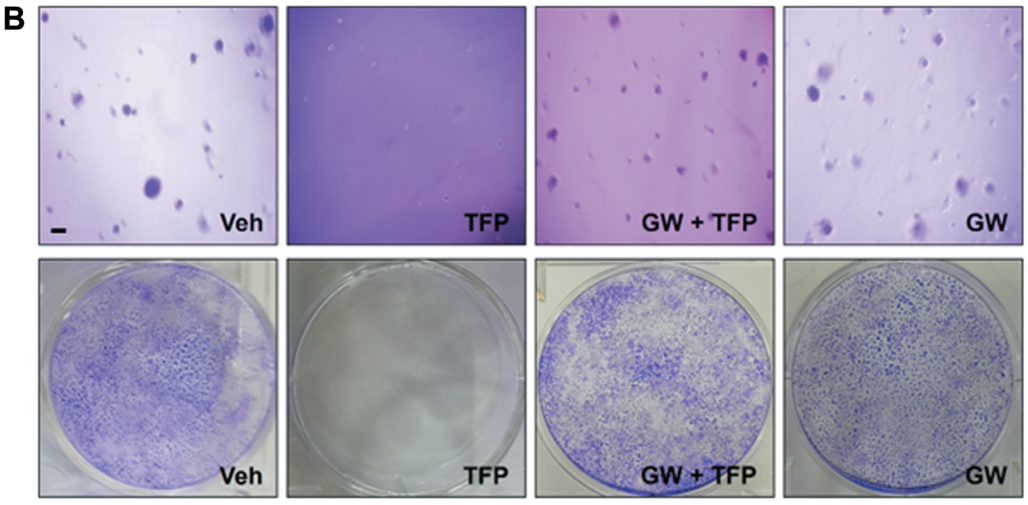

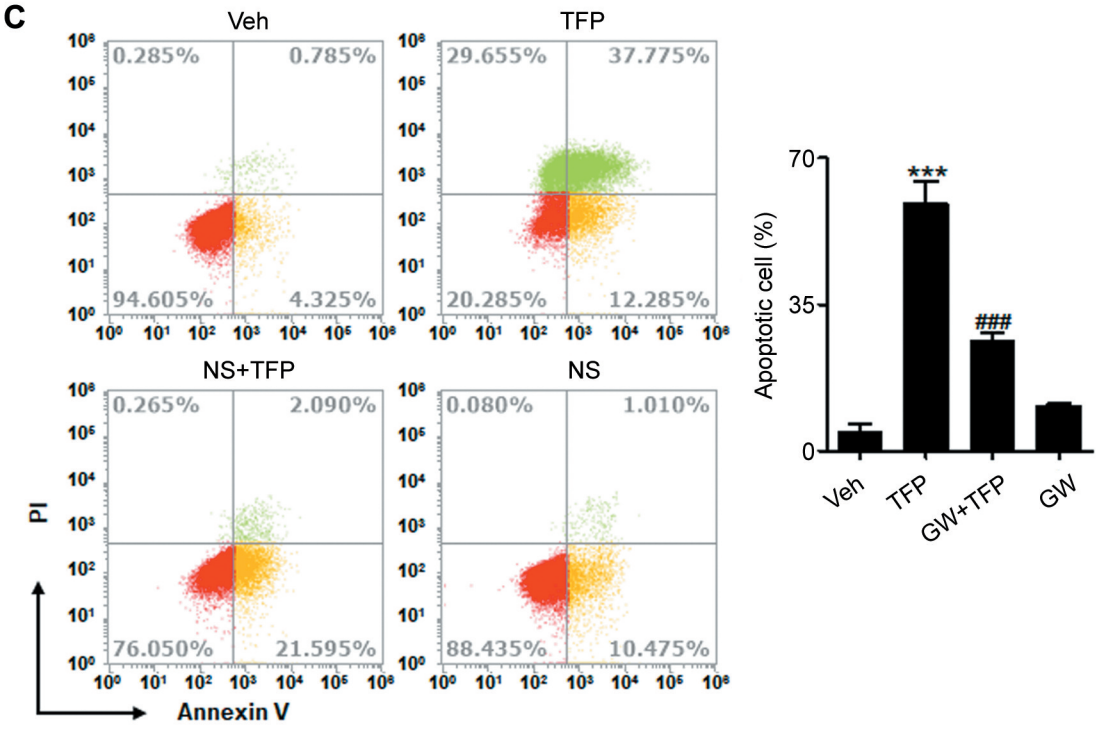

effectively blocked the increase in TFP-induced PG release as well as the nuclear translocation of PPARγ.

In several reports, COX-2-dependent activation of PPARγ was associated with apoptosis (18, 22). However, there are many contradictory results about the role of PPARγ. Thus, we applied a PPARγ inhibitor to test our hypothesis that TFP exerts anti-glioma activity by COX-2-dependent activation of PPARγ. PPARγ inhibitor ameliorated TFP-induced changes in cell viability, colony formation, and apoptotic cell population in U87MG cells.

In conclusion, TFP, at least in part, exerts an anti-cancer effect on GBM through the induction of apoptosis *via* a COX-2/PPARγ-dependent manner.

Conflicts of Interest

The Authors declare that they have no conflicts of interest to report in relation to this study.

Authors' Contributions

Juyeong Park: performed the experiments, collected, and analyzed the data, wrote the manuscript. Joo Yeon Jeong: designed the study, collected, and analyzed the data. Sang Soo Kang: supervised the study, revised the manuscript.

Acknowledgements

The study was supported financially by the National Research Foundation of Korea (NRF) grant funded by the Korean government (MSIT) (No. 2022R1A2C2092464).

References

1 Oronsky B, Reid TR, Oronsky A, Sandhu N and Knox SJ: A review of newly diagnosed glioblastoma. Front Oncol *10*: 574012, 2021. PMID: 33614476. DOI: 10.3389/fonc.2020.574012

2 Würth R, Thellung S, Bajetto A, Mazzanti M, Florio T and Barbieri F: Drug-repositioning opportunities for cancer therapy: novel molecular targets for known compounds. Drug Discov Today *21(1)*: 190-199, 2016. PMID: 26456577. DOI: 10.1016/j.drudis.2015.09.017

3 Rodrigues R, Duarte D and Vale N: Drug repurposing in cancer therapy: influence of patient's genetic background in breast cancer treatment. Int J Mol Sci *23(8)*: 4280, 2022. PMID: 35457144. DOI: 10.3390/ijms23084280

4 Vlachos N, Lampros M, Voulgaris S and Alexiou GA: Repurposing antipsychotics for cancer treatment. Biomedicines *9(12)*: 1785, 2021. PMID: 34944601. DOI: 10.3390/biomedicines9121785

5 Hicks BM, Busby J, Mills K, O'Neil FA, McIntosh SA, Zhang SD, Liberante FG and Cardwell CR: Post-diagnostic antipsychotic use and cancer mortality: a population based cohort study. BMC Cancer *20(1)*: 804, 2020. PMID: 32831062. DOI: 10.1186/s12885-020-07320-3

6 Jeong JY, Park H, Yoo H, Kim EJ, Jeon B, Lee JD, Kang D, Lee CJ, Paek SH, Roh EJ, Yi GS and Kang SS: Trifluoperazine and its analog suppressed the tumorigenicity of non-small cell lung cancer cell; applicability of antipsychotic drugs to lung cancer treatment. Biomedicines *10(5)*: 1046, 2022. PMID: 35625784. DOI: 10.3390/biomedicines10051046

7 Yeh CT, Wu AT, Chang PM, Chen KY, Yang CN, Yang SC, Ho CC, Chen CC, Kuo YL, Lee PY, Liu YW, Yen CC, Hsiao M, Lu PJ, Lai JM, Wang LS, Wu CH, Chiou JF, Yang PC and Huang CY: Trifluoperazine, an antipsychotic agent, inhibits cancer stem cell growth and overcomes drug resistance of lung cancer. Am J Respir Crit Care Med *186(11)*: 1180-1188, 2012. PMID: 23024022. DOI: 10.1164/rccm.201207-1180OC

8 Huang C, Lan W, Fraunhoffer N, Meilerman A, Iovanna J and Santofimia-Castaño P: Dissecting the anticancer mechanism of trifluoperazine on pancreatic ductal adenocarcinoma. Cancers (Basel) *11(12)*: 1869, 2019. PMID: 31769431. DOI: 10.3390/cancers 11121869

9 Xia Y, Xu F, Xiong M, Yang H, Lin W, Xie Y, Xi H, Xue Q, Ye T and Yu L: Repurposing of antipsychotic trifluoperazine for treating brain metastasis, lung metastasis and bone metastasis of melanoma by disrupting autophagy flux. Pharmacol Res *163*: 105295, 2021. PMID: 33176207. DOI: 10.1016/j.phrs.2020.105295

10 Feng Z, Xia Y, Gao T, Xu F, Lei Q, Peng C, Yang Y, Xue Q, Hu X, Wang Q, Wang R, Ran Z, Zeng Z, Yang N, Xie Z and Yu L: The antipsychotic agent trifluoperazine hydrochloride suppresses triple-negative breast cancer tumor growth and brain metastasis by inducing G0/G1 arrest and apoptosis. Cell Death Dis *9(10)*: 1006, 2018. PMID: 30258182. DOI: 10.1038/s41419-018-1046-3

11 Kang S, Hong J, Lee JM, Moon HE, Jeon B, Choi J, Yoon NA, Paek SH, Roh EJ, Lee CJ and Kang SS: Trifluoperazine, a well-known antipsychotic, inhibits glioblastoma invasion by binding to calmodulin and disinhibiting calcium release channel IP3R. Mol Cancer Ther *16(1)*: 217-227, 2017. PMID: 28062709. DOI: 10.1158/1535-7163.MCT-16-0169-T

12 Kang S, Lee JM, Jeon B, Elkamhawy A, Paik S, Hong J, Oh SJ, Paek SH, Lee CJ, Hassan AHE, Kang SS and Roh EJ: Repositioning of the antipsychotic trifluoperazine: Synthesis, biological evaluation and *in silico* study of trifluoperazine analogs as anti-glioblastoma agents. Eur J Med Chem *151*: 186-198, 2018. PMID: 29614416. DOI: 10.1016/j.ejmech.2018.03.055

13 Na HK, Inoue H and Surh YJ: ET-18-O-CH3-induced apoptosis is causally linked to COX-2 upregulation in H-ras transformed human breast epithelial cells. FEBS Lett *579(27)*: 6279-6287, 2005. PMID: 16253239. DOI: 10.1016/j.febslet.2005.09.094

14 Hinz B, Ramer R, Eichele K, Weinzierl U and Brune K: Up-regulation of cyclooxygenase-2 expression is involved in R(+)-methanandamide-induced apoptotic death of human neuroglioma cells. Mol Pharmacol *66(6)*: 1643-1651, 2004. PMID: 15361550. DOI: 10.1124/mol.104.002618

15 Ramer R, Heinemann K, Merkord J, Rohde H, Salamon A, Linnebacher M and Hinz B: COX-2 and PPAR-γ confer cannabidiol-induced apoptosis of human lung cancer cells. Mol Cancer Ther *12(1)*: 69-82, 2013. PMID: 23220503. DOI: 10.1158/1535-7163.MCT-12-0335

16 Sertznig P, Seifert M, Tilgen W and Reichrath J: Present concepts and future outlook: function of peroxisome proliferator-activated receptors (PPARs) for pathogenesis, progression, and therapy of cancer. J Cell Physiol *212(1)*: 1-12, 2007. PMID: 17443682. DOI: 10.1002/jcp.20998

17 Elrod HA and Sun SY: PPARgamma and apoptosis in cancer. PPAR Res *2008*: 704165, 2008. PMID: 18615184. DOI: 10.1155/2008/704165

18 Han SW and Roman J: Anticancer actions of PPARγ ligands: Current state and future perspectives in human lung cancer. World J Biol Chem *1(3)*: 31-40, 2010. PMID: 21537367. DOI: 10.4331/wjbc.v1.i3.31
19 Knopfová L and Smarda J: The use of Cox-2 and PPARγ signaling in anti-cancer therapies. Exp Ther Med *1(2)*: 257-264, 2010. PMID: 22993537. DOI: 10.3892/etm_00000040
20 Xu Z, Choudhary S, Voznesensky O, Mehrotra M, Woodard M, Hansen M, Herschman H and Pilbeam C: Overexpression of COX-2 in human osteosarcoma cells decreases proliferation and increases apoptosis. Cancer Res *66(13)*: 6657-6664, 2006. PMID: 16818639. DOI: 10.1158/0008-5472.CAN-05-3624
21 Eichele K, Ramer R and Hinz B: R(+)-methanandamide-induced apoptosis of human cervical carcinoma cells involves a cyclooxygenase-2-dependent pathway. Pharm Res *26(2)*: 346-355, 2009. PMID: 19015962. DOI: 10.1007/s11095-008-9748-3
22 Walther U, Emmrich K, Ramer R, Mittag N and Hinz B: Lovastatin lactone elicits human lung cancer cell apoptosis *via* a COX-2/PPARγ-dependent pathway. Oncotarget *7(9)*: 10345-10362, 2016. PMID: 26863638. DOI: 10.18632/oncotarget.7213
23 Jing Z, Yu W, Li A, Chen X, Chen Y and Chen J: Trifluoperazine synergistically potentiates bortezomib-induced anti-cancer effect in multiple myeloma *via* inhibiting P38 MAPK/NUPR1. Tohoku J Exp Med *257(4)*: 315-326, 2022. PMID: 35644544. DOI: 10.1620/tjem.2022.J044
24 Hu L, Zhang X, Wang J, Wang S, Amin HM and Shi P: Involvement of oncogenic tyrosine kinase NPM-ALK in trifluoperazine-induced cell cycle arrest and apoptosis in ALK$^+$ anaplastic large cell lymphoma. Hematology *23(5)*: 284-290, 2018. PMID: 29086626. DOI: 10.1080/10245332.2017.1396045
25 Xia Y, Jia C, Xue Q, Jiang J, Xie Y, Wang R, Ran Z, Xu F, Zhang Y and Ye T: Antipsychotic drug trifluoperazine suppresses colorectal cancer by inducing G0/G1 arrest and apoptosis. Front Pharmacol *10*: 1029, 2019. PMID: 31572198. DOI: 10.3389/fphar.2019.01029
26 Chou FH, Tsai KY, Su CY and Lee CC: The incidence and relative risk factors for developing cancer among patients with schizophrenia: a nine-year follow-up study. Schizophr Res *129(2-3)*: 97-103, 2011. PMID: 21458957. DOI: 10.1016/j.schres.2011.02.018
27 Cowdry RW and Gardner DL: Pharmacotherapy of borderline personality disorder. Alprazolam, carbamazepine, trifluoperazine, and tranylcypromine. Arch Gen Psychiatry *45(2)*: 111-119, 1988. PMID: 3276280. DOI: 10.1001/archpsyc.1988.01800260015002
28 Brosius SN, Turk AN, Byer SJ, Longo JF, Kappes JC, Roth KA and Carroll SL: Combinatorial therapy with tamoxifen and trifluoperazine effectively inhibits malignant peripheral nerve sheath tumor growth by targeting complementary signaling cascades. J Neuropathol Exp Neurol *73(11)*: 1078-1090, 2014. PMID: 25289889. DOI: 10.1097/NEN.0000000000000126
29 Pulkoski-Gross A, Li J, Zheng C, Li Y, Ouyang N, Rigas B, Zucker S and Cao J: Repurposing the antipsychotic trifluoperazine as an antimetastasis agent. Mol Pharmacol *87(3)*: 501-512, 2015. PMID: 25552486. DOI: 10.1124/mol.114.096941
30 Yuan K, Yong S, Xu F, Zhou T, McDonald JM and Chen Y: Calmodulin antagonists promote TRA-8 therapy of resistant pancreatic cancer. Oncotarget *6(28)*: 25308-25319, 2015. PMID: 26320171. DOI: 10.18632/oncotarget.4490
31 Raymond JJ, Robertson DM, Dinsdale HB and Nag S: Pharmacological modification of blood-brain barrier permeability following a cold lesion. Can J Neurol Sci *11(4)*: 447-451, 1984. PMID: 6518427. DOI: 10.1017/s0317167100045984
32 Vandonselaar M, Hickie RA, Quail JW and Delbaere LT: Trifluoperazine-induced conformational change in Ca(2+)-calmodulin. Nat Struct Biol *1(11)*: 795-801, 1994. PMID: 7634090. DOI: 10.1038/nsb1194-795
33 Chen QY, Wu LJ, Wu YQ, Lu GH, Jiang ZY, Zhan JW, Jie Y and Zhou JY: Molecular mechanism of trifluoperazine induces apoptosis in human A549 lung adenocarcinoma cell lines. Mol Med Rep *2(5)*: 811-817, 2009. PMID: 21475906. DOI: 10.3892/mmr_00000177
34 Choi H, Chaiyamongkol W, Doolittle AC, Johnson ZI, Gogate SS, Schoepflin ZR, Shapiro IM and Risbud MV: COX-2 expression mediated by calcium-TonEBP signaling axis under hyperosmotic conditions serves osmoprotective function in nucleus pulposus cells. J Biol Chem *293(23)*: 8969-8981, 2018. PMID: 29700115. DOI: 10.1074/jbc.RA117.001167
35 Leger DY, Liagre B, Corbière C, Cook-Moreau J and Beneytout JL: Diosgenin induces cell cycle arrest and apoptosis in HEL cells with increase in intracellular calcium level, activation of cPLA2 and COX-2 overexpression. Int J Oncol *25(3)*: 555-562, 2004. PMID: 15289856.
36 Li MH, Jang JH and Surh YJ: Nitric oxide induces apoptosis *via* AP-1-driven upregulation of COX-2 in rat pheochromocytoma cells. Free Radic Biol Med *39(7)*: 890-899, 2005. PMID: 16140209. DOI: 10.1016/j.freeradbiomed.2005.05.015
37 Pytlowany M, Strosznajder JB, Jeśko H, Cakała M and Strosznajder RP: Molecular mechanism of PC12 cell death evoked by sodium nitroprusside, a nitric oxide donor. Acta Biochim Pol *55(2)*: 339-347, 2008. PMID: 18560609.
38 Gao L, Wang TH, Chen CP, Xiang JJ, Zhao XB, Gui RY and Liao XH: Targeting COX-2 potently inhibits proliferation of cancer cells *in vivo* but not *in vitro* in cutaneous squamous cell carcinoma. Transl Cancer Res *10(5)*: 2219-2228, 2021. PMID: 35116540. DOI: 10.21037/tcr-20-3527
39 Wang Q, Lu D, Fan L, Li Y, Liu Y, Yu H, Wang H, Liu J and Sun G: COX-2 induces apoptosis-resistance in hepatocellular carcinoma cells *via* the HIF-1α/PKM2 pathway. Int J Mol Med *43(1)*: 475-488, 2019. PMID: 30365092. DOI: 10.3892/ijmm.2018.3936
40 Turini ME and DuBois RN: Cyclooxygenase-2: a therapeutic target. Annu Rev Med *53*: 35-57, 2002. PMID: 11818462. DOI: 10.1146/annurev.med.53.082901.103952
41 Föller M, Kasinathan RS, Duranton C, Wieder T, Huber SM and Lang F: PGE2-induced apoptotic cell death in K562 human leukaemia cells. Cell Physiol Biochem *17(5-6)*: 201-210, 2006. PMID: 16790996. DOI: 10.1159/000094125
42 Huang SK, White ES, Wettlaufer SH, Grifka H, Hogaboam CM, Thannickal VJ, Horowitz JC and Peters-Golden M: Prostaglandin E(2) induces fibroblast apoptosis by modulating multiple survival pathways. FASEB J *23(12)*: 4317-4326, 2009. PMID: 19671668. DOI: 10.1096/fj.08-128801
43 Chen YC, Shen SC and Tsai SH: Prostaglandin D(2) and J(2) induce apoptosis in human leukemia cells *via* activation of the caspase 3 cascade and production of reactive oxygen species. Biochim Biophys Acta *1743(3)*: 291-304, 2005. PMID: 15843042. DOI: 10.1016/j.bbamcr.2004.10.016

Received October 6, 2022
Revised October 10, 2022
Accepted October 11, 2022